

# Molecular Mechanisms of Additive Fortification in Model Epoxy Resins: A Solid State NMR Study

Christoph F. Kins,<sup>‡</sup> Dmytro Dudenko,<sup>‡,§</sup> Daniel Sebastiani,<sup>§</sup> and Gunther Brunklaus<sup>\*,‡</sup>

<sup>‡</sup>Max-Planck-Institut für Polymerforschung, Postfach 31 48, D-55021 Mainz, Germany, and <sup>§</sup>Freie Universität Berlin, Arnimallee 14, D-14195 Berlin, Germany

Received June 22, 2010; Revised Manuscript Received July 23, 2010

**ABSTRACT:** The bulk properties of polymers are often adjusted via addition of a complex blend of compounds collectively known as additives, where so-called molecular fortifiers (or *antiplasticizers*) may improve the mechanical properties. In the present work, insight into molecular mechanisms of additive-fortification in model epoxy resins was obtained from multinuclear solid-state NMR analysis. In particular, we have demonstrated a “free molecule”-type behavior of DMSO-*d*<sub>6</sub> in DMSO-fortified resins similar to common inclusion compounds thereby revealing mere filling of free volume. In case of DMMP-fortified resins, however, chemical modification during postcure of the epoxy resin is observed yielding methyl methylphosphonate (MMP) and salt formation, where dynamic heterogeneities of MMP-*d*<sub>3</sub> suggest a rather complex mechanism of fortification. The interpretation of NMR data was further supported by *ab initio* calculations.

## 1. Introduction

The bulk properties of polymers are often adjusted via addition of a complex blend of compounds collectively known as additives that facilitate a broad range of applications.<sup>1</sup> To date, many categories of additives such as fillers, antioxidants, plasticizers, flame retardants, and stabilizers, are known. While plasticizers typically soften the resulting material rendering it more flexible, a rather unique class of additives (so-called molecular fortifiers or antiplasticizers) may improve the mechanical properties of polymers yielding increased modulus and tensile strength. However, addition of fortifiers is only possible up to a system-dependent weight limit above which the polymer is replasticized. Notably, no generally accepted mechanism of fortification is known to date although a variety of polymeric systems such as epoxy resins,<sup>2–7</sup> poly(sulfone ether),<sup>8</sup> cellulose triacetate,<sup>8</sup> polycarbonate,<sup>9</sup> poly(styrene),<sup>10</sup> poly(vinyl chloride)<sup>11</sup> and poly(ethylene terephthalate)<sup>12</sup> have been studied. Nevertheless, in all cases, fortification is believed to result from *non-covalent* interactions of the respective additive with the polymer host matrix.<sup>13</sup> Since often the polymer density is increased markedly, mere filling of *free volume* by the additive has been proposed and in some cases supported by either reduced gas permeabilities<sup>14,15</sup> or xenon gas sorption experiments.<sup>16</sup> Furthermore, fortification commonly comprises a reduction of both the glass transition temperature  $T_G$  and magnitude of the high temperature part of the secondary loss transition (i.e.,  $\beta$ -transition), as revealed by dynamic mechanical or dielectric measurements.<sup>2,4,5,7,9,14,17,18</sup> In addition, occupancy of free volume by additives can restrict local motions of structural units or larger fragments thus reflecting molecular interactions with the host.

In the present work, we explore the molecular origin of fortification of a recently introduced bisphenol A based model epoxy resin upon addition of either dimethyl sulfoxide (DMSO) or dimethyl methyl phosphonate (DMMP) (Scheme 1a) utilizing modern solid-state NMR, which has been shown to be a powerful

tool for the analysis of local motions of moieties,<sup>19</sup> e.g., in polymer/diluent systems,<sup>20</sup> providing an outstanding selectivity for local environments even in rather ill-defined compounds.<sup>21</sup> Particularly, solid-state NMR techniques such as temperature-dependent proton spin–lattice relaxation in the rotating frame,<sup>22,23</sup> <sup>13</sup>C spin diffusion,<sup>24</sup> <sup>2</sup>H spin echo,<sup>25–28</sup> chemical shift anisotropy<sup>28–31</sup> or multinuclear REDOR NMR<sup>32</sup> measurements have been successfully applied.

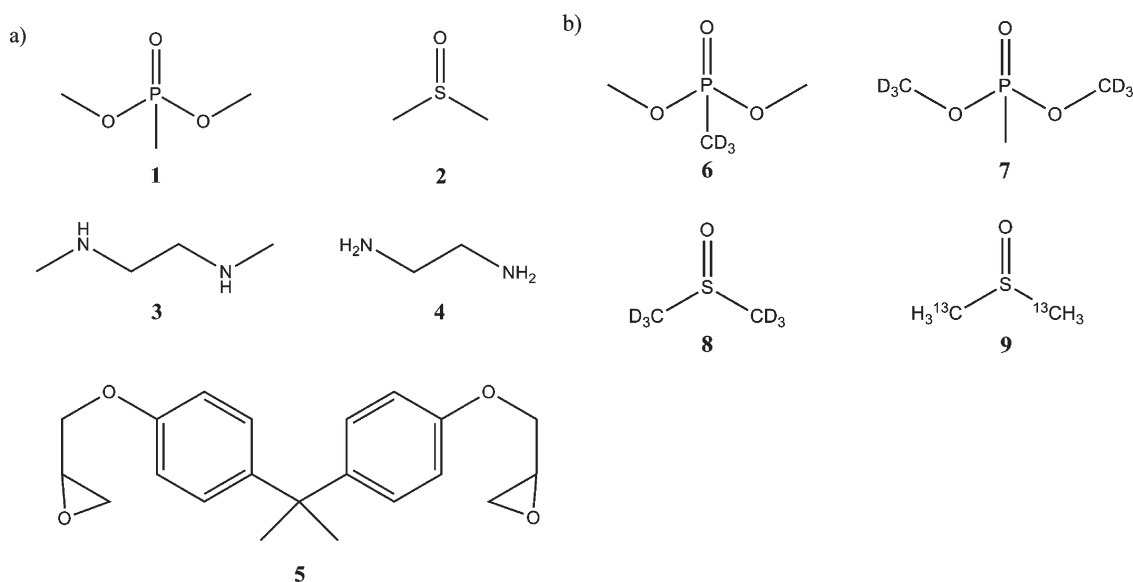
Although DMSO and DMMP have fairly comparable molecular structures and fortifying characteristics (up to approximately 15 mol %), they differ markedly in their impact on both the thermal and dynamic mechanical relaxation properties of the considered model epoxy network. Using selectively <sup>2</sup>H- and/or <sup>15</sup>N-labeled fortifiers or curing agents, we could demonstrate that DMSO indeed shows a “free molecule”-type behavior while DMMP reacts with the polymer backbone via methylation of amino functionalities (Scheme 2)<sup>33</sup> thereby leading to salt formation. Notably, interpretation of the NMR data was facilitated by both a nucleus independent chemical shift (NICS) map<sup>34</sup> and *ab initio* density functional theory (DFT)<sup>35</sup> chemical shift computations of corresponding snapshot geometries derived from Car–Parrinello molecular dynamics (CPMD) simulations.

## 2. Experimental Section

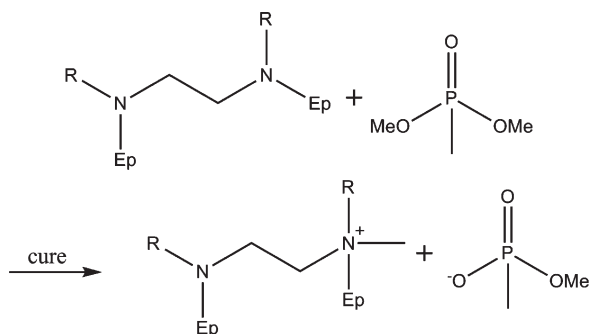
**Network Fabrication.** The epoxy resins were prepared as described.<sup>17</sup> Four parts of epoxy monomer Epon 825 (a bisphenol A diglycidylether supplied by Miller Stephenson Chemical, USA) were heated to 50 °C for better processability by reducing its viscosity. Then, two parts of dimethyl ethylenediamine, one part of ethylenediamine and, if required, 1.23 parts (corresponding to 15 mol % of the total amount of monomers used and slightly less than one fortifier molecule per three bisphenol A units) of fortifier were added and mixed at 50 °C until a homogeneous solution was obtained. Subsequently, the mixture was precured at 50 °C for 3 h, followed by a postcuring at 110 °C for 16 h to ensure full conversion. Ethylenediamine was purchased from Acros; dimethyl ethylenediamine and DMSO were obtained from Sigma-Aldrich while DMMP was

\*Corresponding author. E-mail: brunklaus@mpip-mainz.mpg.de.

**Scheme 1.** (a) Structures of Fortifiers DMMP (1) and DMSO (2), Amine Monomers Dimethyl Ethylenediamine (3) and Ethylenediamine (4) as well as the Epoxy Resin Bisphenol A Diglycidyl Ether (Epon 825) (5) and (b) Structures of Selectively Isotope Labeled Fortifiers Dimethyl Methyl- $d_3$  Phosphonate (6), Dimethyl- $d_6$  Methylphosphonate (7), Dimethyl Sulfoxide- $d_6$  (8) and Dimethyl- $^{13}C_2$  Sulfoxide (9)



**Scheme 2.** Representative Cutout of the Polymer Backbone Reacting with DMMP During Cure Process<sup>a</sup>



<sup>a</sup> Ep is short for a bisphenol A diglycidyl ether residue attached to an amino functionality by epoxy ring-opening. In case of dimethyl ethylenediamine or ethylene diamine, R = CH<sub>3</sub> or R = Ep respectively.

delivered from Alfa Aesar. All compounds were used as-obtained without further purification.

**Deuteration of Amines.** First, 7.00 mL of ethylenediamine (6.29 g, 105 mmol) or 7.00 mL of *N,N'*-dimethyl ethylenediamine (5.74 g, 65 mmol) respectively had been mixed with 50 mL of methanol-*d* and heated under reflux for 6 days under an argon atmosphere before methanol was removed for the most part by distillation. <sup>1</sup>H NMR revealed a degree of deuteration of approximately 60% of the amino functionality by integration of the respective proton resonance. The procedure was repeated by adding 50 mL of fresh methanol-*d* to the crude product and refluxing the mixture for additional 6 days under argon atmosphere. Subsequent thorough distillation yielded amine with a degree of deuteration ranging from 90 to 95% as revealed by <sup>1</sup>H NMR. This was double-checked by measuring <sup>2</sup>H NMR spectra with DMSO-*d*<sub>6</sub> as internal reference. Care was taken to keep the residual methanol content below 1 mol % as monitored by <sup>1</sup>H NMR.

**Preparation of Dimethyl Methyl-*d*<sub>3</sub> Phosphonate.** First, 2.15 mL of iodomethane-*d*<sub>3</sub> (5.00 g, 34.5 mmol) and 1.02 mL of trimethyl phosphite (1.07 g, 8.6 mmol), corresponding to a 4-fold excess of iodomethane-*d*<sub>3</sub>, were mixed and refluxed under argon atmosphere overnight. <sup>1</sup>H NMR indicated full conversion of trimethyl phosphite. Distillation at 60 °C (11 mbar) yielded 0.71 mL (0.8 g, 6.4 mmol, 74%) of dimethyl methyl-*d*<sub>3</sub> phosphonate, and <sup>1</sup>H NMR denoted a degree of deuteration of 90%.

**Preparation of Dimethyl-*d*<sub>6</sub> Methylphosphonate.** A 10.94 mL aliquot of phosphorus trichloride (17.22 g, 125 mmol) in 150 mL of dichloromethane was dropped into a mixture of 49.11 mL *N,N'*-dimethylaniline (46.65 g, 385 mmol) and 15.23 mL of methan-*d*<sub>3</sub>-ol-*d* (13.53 g, 375 mmol) in 75 mL of dichloromethane over 1 h at a temperature of 0 °C. After the mixture was stirred for another hour at room temperature, dichloromethane was roughly removed by distillation. Addition of 200 mL diethyl ether resulted in the formation of two phases and the precipitation of the hydrochloride salt of *N,N'*-dimethylaniline. The suspension was filtered and the transparent liquid distilled at ambient pressure at 140 °C. All that was not collected until 140 °C was discarded. This procedure afforded 3.1 mL (3.3 g, 25 mmol) of trimethyl-*d*<sub>9</sub> phosphite that were added to 9.34 mL of iodomethane (21.29 g, 150 mmol) and refluxed under argon atmosphere overnight. Upon addition of iodomethane, impurities of *N,N'*-dimethylaniline precipitated as quaternary ammonium salt. Distillation yielded 1.4 mL (11% relating to phosphorus trichloride) of dimethyl-*d*<sub>6</sub> methyl phosphonate (1.7 g, 13 mmol). <sup>1</sup>H NMR, <sup>2</sup>H NMR, <sup>31</sup>P NMR revealed that the product is composed of ca. 90% DMMP, and 10% dimethyl hydrogen phosphonate. This byproduct is formed by the reaction of trimethyl phosphite with hydrochloric acid and cannot be separated trivially.

**Labeled Dimethyl Sulfoxide.** Dimethyl-<sup>13</sup>C<sub>2</sub> sulfoxide and dimethyl-*d*<sub>6</sub> sulfoxide were purchased from Sigma-Aldrich and used as received.

**Preparation of Methyl Methyl Phosphonic Acid.** A 1.53 mL aliquot of DMMP (1.76 g, 14.2 mmol) and 5.94 mL of triethylamine (4.31 g, 42.6 mmol) were mixed and stirred thoroughly as two phases (ionic liquid and triethylamine) formed during the course of the reaction. After reflux for 4 days, approximately 80% of the DMMP was demethylated. The upper phase was removed and the lower phase kept at 120 °C and 6 mbar for 1 h to remove residual DMMP. The resulting pure ionic liquid *N,N*-diethyl-*N*-methylethanaminium methyl methylphosphonate is dissolved in water and treated with a strong acidic cation exchange resin (Amberlite IR120). Filtration and distillation of the solution at 15 mbar and 120 °C yields 1.0 g (0.8 mL, 9.2 mmol, 65% yield relating to DMMP) of methyl methylphosphonic acid (MMPA) as a liquid.

**Verification of Samples.** All prepared resins were verified by means of mechanical and thermal analysis (e.g., tensile strength, elastic modulus, glass transition temperature) against reference

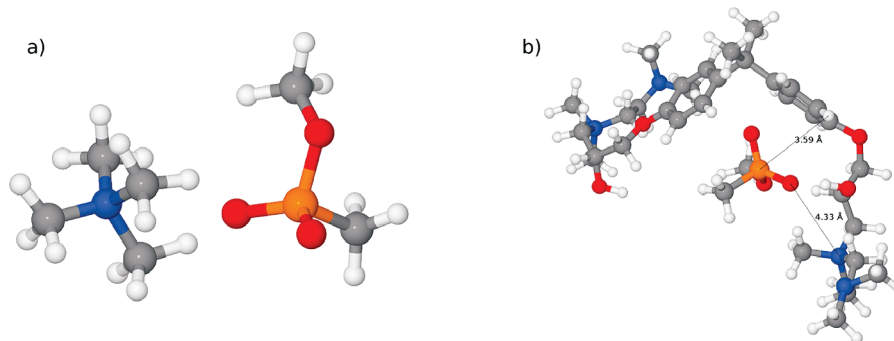


**Figure 1.** (a) “Ionic liquid” of MMP and (b) model cutout of the epoxy resin comprising an aromatic bisphenol A moiety and quaternized nitrogen atoms reflecting salt formation. For simplicity only one MMP counterion is shown. The average distance of the P atom to the closest aromatic proton as well as the shortest average PO $\cdots$ N distance are also given.

compounds from a previous study. Differential scanning calorimetry (DSC) was performed at a heating rate of 10 K/min on as-synthesized resins, i.e. they were not rasped to a powder to obtain values comparable with literature data.<sup>17</sup> Dog bone shaped samples with a width of 4 mm, length of 30 mm and thickness of 2 mm were milled out of an as-synthesized resin. Measurements with a strain rate of 0.63 mm/min were performed with an Instron 6022 tensile testing machine. While the expected trends in both tensile strength and elastic modulus are confirmed, the absolute values are reproducibly 20% below published data<sup>17</sup> which might be attributed to (slightly) different experimental conditions such as the absence of an extensometer due to geometry restrictions. Dynamic mechanical thermal analysis (DMTA) data was collected on an Ares LS from Rheometric Scientific by shearing a single cantilever beam from  $-120$  to  $+150$  °C at a maximum strain of  $\epsilon = 10^{-4}$ , constant frequency of 1 Hz and temperature ramp rate of 2 K/min. As suggested by DSC, the  $\alpha$ -transition is found to be higher for the DMMP modified network than for the neat resin corresponding to a higher glass transition temperature; there is no suppression of the  $\beta$ -relaxation compared to the unfortified network. In contrast, the DMSO fortified resin exhibits the typical suppression of  $\beta$ -relaxation accompanied by a decrease in the  $\alpha$ -transition. This is in accordance with published data.<sup>17</sup> In addition, <sup>13</sup>C CPMAS NMR spectra (which are sensitive to the molecular environment or packing effects in solids and thus may be considered as representative “fingerprints”)<sup>36</sup> of the neat and DMSO- or DMMP-fortified resins were acquired. Notably, all <sup>13</sup>C CPMAS spectra of our self-synthesized resins showed excellent agreement with the corresponding spectra of original resins prepared by Lesser et al.,<sup>17</sup> thus confirming the identity of the samples. All reference compounds were kindly provided by M. Junk.

### 3. Computational Section

It is well-known that a reliable computation of NMR parameters (like absolute chemical shielding) crucially depends on the chemical environment of considered atoms and fragments. While highly accurate electronic structure methods on an explicitly correlated level of theory are available for the calculation of structures and NMR properties of relatively small molecular systems, density functional theory represents a compromise between accuracy and computational efficiency and has been proven to yield sufficient agreement with experimental data.

Figure 1a shows a simplified “ionic liquid” model of MMP while Figure 1b displays a “non-branched” model cutout of the epoxy resin comprising a bisphenol A moiety with two quaternized (methylated) nitrogen atoms whose positive charges are compensated by two MMP anions. The latter illustrates a possible inclusion of the fortifier within the resin matrix. Since the bulk organization of the investigated epoxy resin is not known, all CPMD simulations were conducted for isolated model clusters

thereby neglecting the backbone chains. Since NMR data provides information on *local* interactions, we believe that this rather simplified “non-branched” model is in principle able to demonstrate the actual host–guest interplay thereby reflecting the experimental observations including changes of <sup>31</sup>P isotropic absolute chemical shieldings before and after the salt formation between the host and respective guest molecules. Both model systems were stepwise “heated” until 350 K performing at least 1 ps of molecular dynamics simulation for each temperature step of 50 K. The total “heating” time was 7 ps followed by a production run of 4 ps. All calculations were carried out with the CPMD<sup>37</sup> package in the framework of DFT using the gradient-corrected exchange and correlation functionals (BLYP),<sup>38,39</sup> Goedecker-type pseudopotentials<sup>40</sup> together with a plane wave cutoff of 70 Ry.

For analysis of possible NMR chemical shift effects resulting from trapping of a fortifier molecule (DMMP or MMP) in proximity to the aromatic bisphenol A moiety, a single NICS map<sup>41</sup> calculation of the host structure was performed (Figure 7). In short, the NICS map displays how much the local magnetic fields are shielded (or deshielded) by the host moiety providing a qualitative approach to experimentally observed shift effects. For both models, the averaged isotropic absolute chemical shieldings were computed on a subset of configurations extracted from the corresponding CPMD production trajectories. Typically 40 randomly selected snapshots were sampled for each model system and used for NMR chemical shift computations employing the Gaussian03 program package<sup>42</sup> with B3LYP exchange-correlation functional<sup>43</sup> and the relatively large 6-311++G(3d2f,3p2d) basis set for phosphorus atoms, while all other atoms were described by the 6-31+G(d,p) basis set.

## 4. Results and Discussion

**4.1. Proton NMR.** In a previous report, the effects of DMMP on the host polymer were attributed to hydrogen bonding of the resin’s hydroxyl protons with the P=O double bond of DMMP.<sup>13,17</sup> Indeed, the respective X=O groups (X = P, S) of both additives constitute possible hydrogen-bond acceptors, as it is well-known that not only DMSO exhibits strong interactions with hydrogen donors<sup>44–48</sup> but also 1:1 hydrogen-bonded complexes of water and DMMP have been reported.<sup>49,50</sup> Protons involved in hydrogen-bonded structures<sup>51</sup> often exhibit well-resolved <sup>1</sup>H chemical shifts and can be identified by <sup>1</sup>H MAS NMR.<sup>52</sup> Even in case of dynamic hydrogen-bonding, i.e. exchange of the proton among two heavy atoms with a given distance,<sup>53</sup> the “effective strength” of the hydrogen bond can be obtained: typical evidence of strong hydrogen bonding are high-frequency shifted <sup>1</sup>H resonances, i.e., at 16–22 ppm for hydrogen-bonds to nitrogen or oxygen.<sup>54</sup>

An inspection of the <sup>1</sup>H fast MAS NMR spectra (cf. Figure 2), however, reveals no *obvious* indication of strong

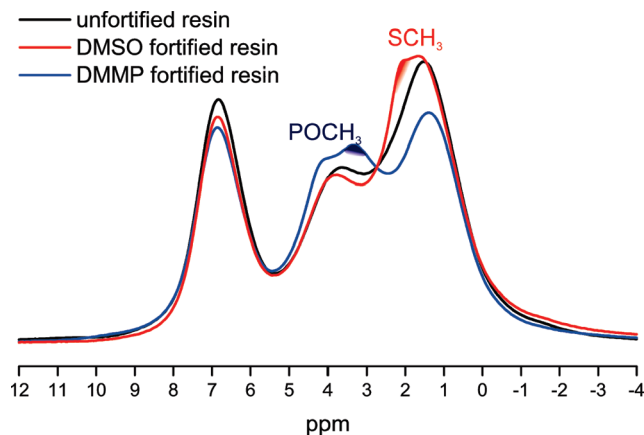


**Figure 2.**  $^1\text{H}$  MAS NMR spectra of the unfortified, DMSO and DMMP fortified epoxy resin, acquired at 850.1 MHz using a commercially available Bruker 1.3 mm double-resonance MAS probe at a spinning frequency of 50 kHz, typical  $\pi/2$ -pulse lengths of 2  $\mu\text{s}$  and recycle delays of 5–10 s coadding 32 transients. Note the barely resolved  $\text{POCH}_3$  resonance at 3.3 ppm and  $\text{DMSO-SCH}_3$  resonance at 2.1 ppm, respectively.

hydrogen-bonding. Nevertheless, according to *ab initio* DFT  $^1\text{H}$  chemical shift computations of a tentative model geometry, the presence of fairly weak  $\text{OH}\cdots\text{O}=\text{P}$  hydrogen bonds is likely. The hydroxyl proton resonance was computed at  $\delta(^1\text{H}) \approx 7$  ppm and therefore may be buried under the broad resonances of aromatic moieties of the host polymer, but admittedly, successful enhancement of *mechanical* properties does not solely depend on hydrogen-bonding as numerous fortifier/polymer systems are known where this can be ruled out based on rather simple structural considerations.<sup>6,10,11</sup>

$^1\text{H}$ - $^1\text{H}$  double-quantum (DQ) MAS NMR<sup>55</sup> is in general a highly useful and selective approach to identify close contacts or spatial proximities of different structural moieties, e.g. upon successful molecular recognition,<sup>56</sup> while local ordering of both the epoxy resin and fortifier during cure may be also identified from spin-diffusion<sup>24</sup> or REDOR experiments.<sup>32</sup> In the aforementioned  $^1\text{H}$ - $^1\text{H}$  two-dimensional experiment, DQ coherences due to pairs of dipolar coupled protons are correlated with single-quantum coherences resulting in characteristic correlation peaks. Double-quantum coherences between *like* spins appear as a single correlation peak on the diagonal, while a pair of cross peaks that are symmetrically arranged on either side of the diagonal reflects couplings among *unlike* spins. In addition, at short dipolar recoupling times (i.e., 20–40  $\mu\text{s}$ ), observable DQ signal intensities are proportional to  $D_{ij}^2$  or  $r_{ij}^{-6}$ , ( $D_{ij}$  is the homonuclear dipolar coupling constant,  $r_{ij}$  the internuclear distance), respectively, so that strong signal intensities in the corresponding DQ MAS NMR spectrum indicate protons in rather close spatial proximity (i.e., up to 3.5 Å).<sup>57</sup> In contrast, rather weak DQ signals reflect either long-distance contacts or the presence of fast local molecular dynamics (with respect to the time scale of the experiment).<sup>58</sup> The  $^1\text{H}$ - $^1\text{H}$  DQ MAS NMR spectrum of the DMMP fortified epoxy resin is displayed in Figure 3; the experiment was performed at a high spinning frequency of 50 kHz in order to maximize the achievable spectral resolution in the indirect dimension (F1) of the experiment. Three DQ peaks between like spins can be identified which are assigned to the methyl group protons of the bisphenol A moiety (BPA; 1.3 ppm), the aliphatic region of the polymer backbone (2.5–4.0 ppm) and the aromatic protons of BPA (6.7 ppm). These are rather trivial DQ peaks merely reflecting the molecular structure of the polymer. In contrast, the DQ crosspeak at 10.0 ppm = 6.7 +

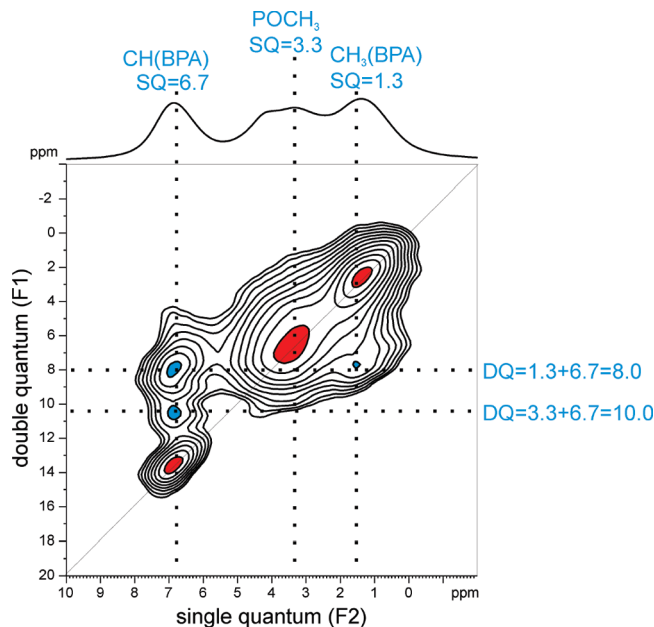


**Figure 3.**  $^1\text{H}$ - $^1\text{H}$  DQ MAS NMR spectrum of DMMP fortified resin at 850.1 MHz and 50 kHz MAS, acquired under the following experimental conditions:  $\tau_{\text{exc}} = 20 \mu\text{s}$ , 128  $t_1$  increments at steps of 20.0  $\mu\text{s}$ , relaxation delay 5 s, 16 transients per increment. Twelve positive contour levels between 12% and 95% of the maximum peak intensity were plotted. The  $F_2$  projection is shown on the top. The back-to-back (BaBa)<sup>59</sup> recoupling sequence was used to excite and reconvert double-quantum coherences, applying States-TPPI<sup>60</sup> for phase sensitive detection. DQ peaks between like or unlike spins are colored in red and blue, respectively.

3.3 ppm suggests close contact of the fortifier- $\text{OCH}_3$  units (3.3 ppm) to the aromatic BPA moieties. Notably, similarly recorded  $^1\text{H}$  DQ MAS NMR spectra of both the unfortified and DMSO fortified resin did not show a DQ cross peak at 10.0 ppm, hence excluding an alternate assignment of the peak at around 3 ppm to the aliphatic parts of the polymer backbone (see Supporting Information). However, selective DQ crosspeaks of DMSO and the host polymer could not be resolved. A preferential location of the phosphonate-based fortifier is indeed consistent with previous studies of polycarbonate,<sup>26</sup> polyethylene terephthalate (PET)<sup>28</sup> and aryl aliphatic epoxy resins<sup>23</sup> where a substantial reduction of the phenyl flip rate upon incorporation of the fortifier was observed.

**4.2.  $^{13}\text{C}$  NMR and 2D  $^1\text{H}$ - $^{13}\text{C}$  correlation NMR.** The  $^{13}\text{C}$  CPMAS spectra of the unfortified and fortified resins are shown in Figure 4. In all cases, the aromatic region (100 ppm–180 ppm) is virtually identical while—apart from individual peaks of the respective fortifier molecules—distinct but small differences in the aliphatic region (45–90 ppm) in the case of DMMP fortified resin can be found. In contrast, the similarity of the corresponding  $^{13}\text{C}$  CPMAS spectra of both DMSO and unfortified resin indicate a rather negligible influence of DMSO on the local structure of the polymer host. However, the S- $\text{CH}_3$  units of DMSO cannot be resolved unless preparing a fortified resin using  $^{13}\text{C}$ -labeled DMSO. In that case, a fairly sharp peak at 40.8 ppm (which is close to the resonance frequency of pure DMSO)<sup>61</sup> is obtained where the peak width of about 47 Hz hints at fast rotational motions. In contrast, the peak width of the resolved P- $\text{CH}_3$  resonance centered at about 13 ppm is much broader (450 Hz) and suggests either an ill-defined local environment or hindered local mobility. Similarly, a rather broad peak for the P- $\text{OCH}_3$  unit at  $\approx 52$  ppm is

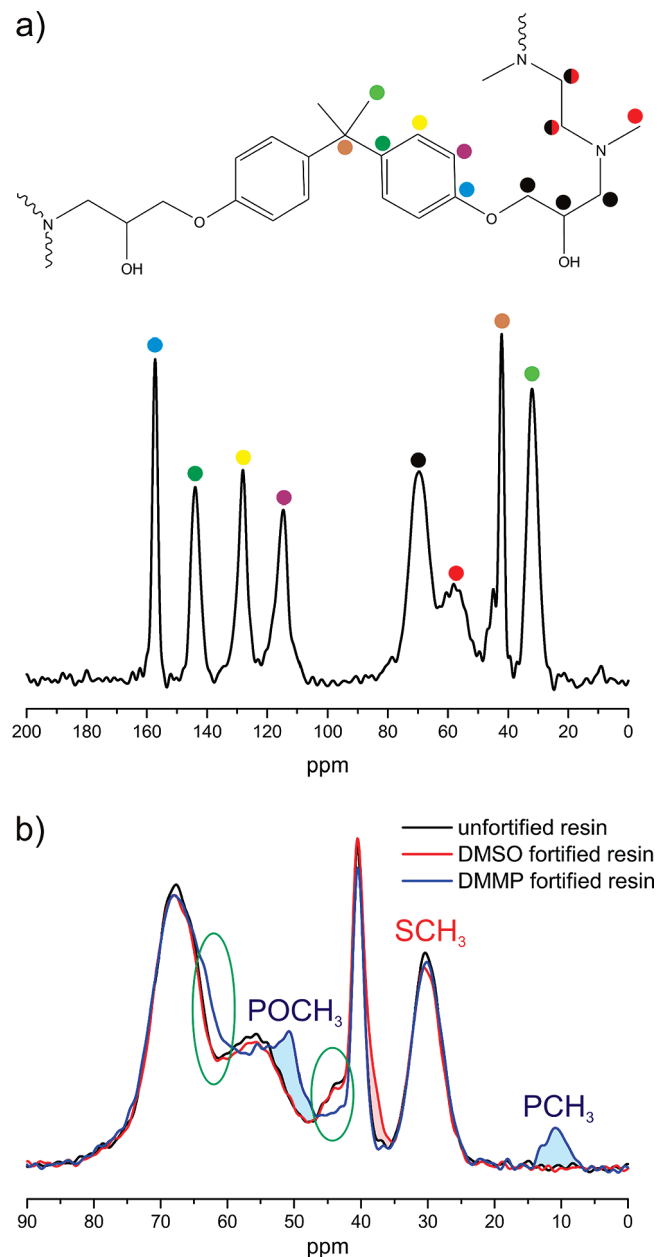


**Figure 4.** (a)  $^{13}\text{C}$  CP-MAS spectrum of the unfortified resin with peak assignment. Because of local symmetry of the bisphenol A moiety, both aromatic units attached to the quaternary carbon appear equivalent. (b) Stack plot of the  $^{13}\text{C}$  CP-MAS spectra (region 0–90 ppm) of unfortified and DMSO or DMMP fortified resins. Noticeable differences in case of DMMP fortified resin are marked by green circles, and resonances assigned to the respective fortifier are shaded. All spectra were acquired at 125.77 MHz using a Bruker DSX 500 machine with a contact time of 2 ms coadding 6144 transients. The experiments were carried out using a Bruker 2.5 mm double resonance MAS probe spinning at 25 kHz, a  $\pi/2$ -pulse length of 2.5  $\mu\text{s}$ , and a recycle delay of 5 s.

observed. In comparison to pure DMMP, both resonances are shifted to higher ppm values (ca. +5 ppm) possibly reflecting packing or conformational effects other than  $\pi$ -shifts associated with aromatic moieties<sup>62</sup> since in comparison to liquid-state NMR chemical shifts, ring current effects typically result in lower ppm values. Notably at temperatures below  $-20^\circ\text{C}$  the aromatic carbon resonances of the bisphenol A moiety at 128 and 115 ppm split into two resonances each, indicating a slowing down of the well-known phenyl flip motion.

In order to identify the possible presence of various P-CH<sub>3</sub> environments and hence fortifier species, we acquired a  $^1\text{H}$ - $^{13}\text{C}$  heteronuclear correlation spectrum applying the rather selective recoupled polarization transfer (REPT) technique that is based on rotational echo double resonance (REDOR)-type recoupling of the otherwise averaged heteronuclear dipolar coupling.<sup>63,64</sup> Specifically, initial  $^1\text{H}$  magnetization is used to create a heteronuclear single-quantum coherence (HSQC), which is subsequently monitored in the indirect dimension ( $t_1$ ) before it is converted to  $^{13}\text{C}$  magnetization that is acquired in the direct dimension ( $t_2$ ). Here, proper setting of the dipolar recoupling time ( $1-8\tau_{\text{R}}$ ; with  $\tau_{\text{R}} = 33.6\mu\text{s}$ ) allows to distinguish both short-range and/or long-range contacts.

The corresponding REPT-HSQC spectrum of DMMP fortified resin is given in Figure 5a, while Figure 5b provides a zoom into the  $^{13}\text{C}$  spectral region of 10–60 ppm, where the (intramolecular) fortifier  $\text{POCH}_3$  and P-CH<sub>3</sub> crosspeaks are highlighted. While no unambiguous crosspeaks between the host matrix and fortifier could be obtained, even at recoupling periods as high as  $8\tau_{\text{R}}$  and a temperature of  $-20^\circ\text{C}$ , two distinct P-CH<sub>3</sub> peaks can be identified suggesting a rather ill-defined fortifier environment. When repeating such correlation experiments with resins fortified with selectively deuterated DMMP (either dimethyl- $d_6$ -methyl phosphonate or dimethyl methyl- $d_3$  phosphonate) the corresponding  $\text{POCH}_3$  or P-CH<sub>3</sub> peaks vanished. Also, in case of unfortified resin, no intensity in the respective spectral region is observed.

**4.2.  $^{31}\text{P}$  NMR and 2D  $^1\text{H}$ - $^{31}\text{P}$  Correlation NMR.** As an independent probe, we acquired a proton decoupled  $^{31}\text{P}$  MAS NMR spectrum of the DMMP-fortified resin. It shows a fairly broad peak centered at 22.7 ppm indicating a chemical shift distribution typically observed in polymeric systems. Most notably, the peak is shifted  $\approx 11$  ppm to lower ppm compared to pristine DMMP, which appears rather unlikely to originate simply from (e.g., aromatic) packing effects (Figure 7). Variable temperature measurements in the range from  $-20$  to  $+100^\circ\text{C}$  yielded significantly narrowed linewidths (1248 Hz at  $-20^\circ\text{C}$ , 222 Hz at  $+100^\circ\text{C}$  at 25 kHz MAS) while the resonance shifts only slightly ( $\Delta\delta = -0.7$  ppm) with increasing temperature, hence suggesting local melting of the network structure and possibly softening of (weaker) hydrogen-bonds. In case of fairly strong hydrogen bonds breaking near the glass transition temperature  $T_{\text{G}}$ , the resonance shift should be considerably larger, which is not observed. Since in other cases of phosphorus-based additive-modified polymer systems a partial aggregation of the additive(s) was proposed,<sup>29,30</sup> possible clustering of DMMP in DMMP-fortified epoxy resin was investigated via a  $^{31}\text{P}$  DQ filtered experiment. In such an experiment, a DQ signal in principle can only be produced if at least two  $^{31}\text{P}$  spins (like or unlike) are coupled. Specifically, the symmetry based  $\text{R14}_6^{\text{D}}$  pulse sequence<sup>65</sup> that reintroduces the homonuclear dipolar coupling under moderately fast MAS was employed at varying recoupling times ranging from 2.4 ms up to 10 ms. However, even at low temperature and a rather long recoupling time, only a faint DQ signal was observed. This finding demonstrates that merely a negligible fraction of fortifier molecules are in close spatial proximity.

In contrast to the  $^1\text{H}$ - $^{13}\text{C}$  REPT-HSQC spectra where no unambiguous contact peaks between both the fortifier and polymer matrix could be identified, a contact peak of the aromatic bisphenol A moiety and the phosphonate can be observed in the respective  $^1\text{H}$ - $^{31}\text{P}$  REPT-HSQC spectra of DMMP fortified resins. In particular, resins fortified with either dimethyl- $d_6$  methyl phosphonate (DMMP- $d_6$ ) or

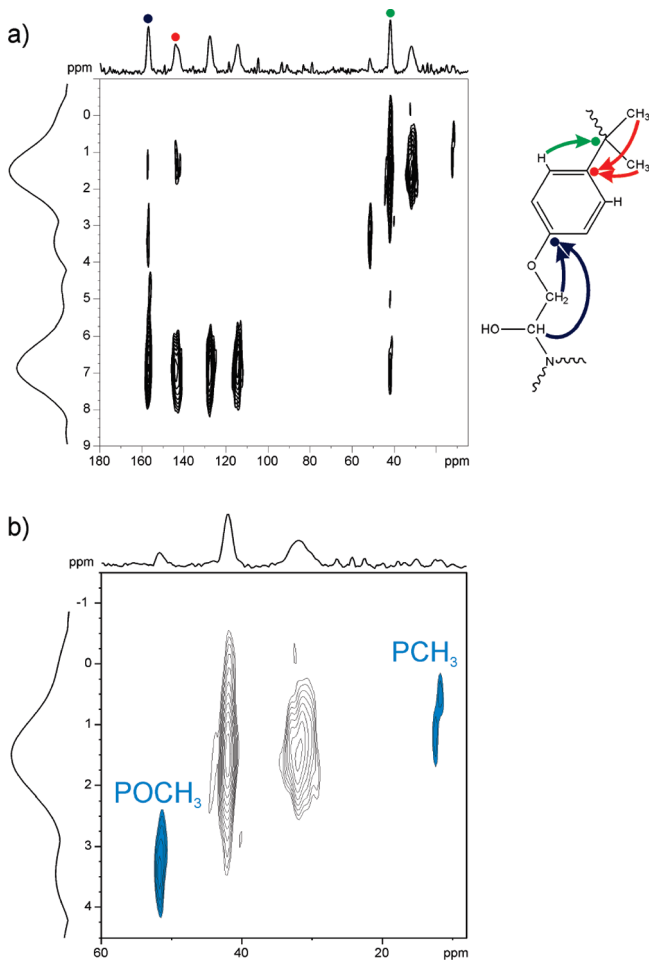


**Figure 5.** (a)  $^1\text{H}$ – $^{13}\text{C}$  REPT–HSQC spectrum of DMMP fortified resin recorded at 850.1 MHz and 29762 Hz MAS using a Bruker Avance III spectrometer with a commercially available Bruker 2.5 mm double-resonance MAS probe,  $\pi/2$ -pulse lengths of 2.5  $\mu\text{s}$  for both  $^1\text{H}$  and  $^{13}\text{C}$  and a recoupling time of  $6\tau_{\text{R}} \approx 0.2$  ms. A total of 24  $t_1$  increments at steps of 33.6  $\mu\text{s}$  ( $=1\tau_{\text{R}}$ ) and 2048 transients per increment have been added with a relaxation delay of 3 s. Eleven positive contour levels between 10% and 90% of the maximum peak intensity are plotted; the  $F_2$  projection is shown on top. In addition to correlation peaks reflecting mere one-bond correlations, more remote couplings between nuclei are also observed. This is illustrated with a representative cutout of the polymer backbone next to the spectrum. Through-space polarization transfer is represented by arrows. (b) Zoom into the spectral region 10–60 ppm. Note the splitting of the P– $\text{CH}_3$  resonance.

dimethyl methyl- $d_3$  phosphonate (DMMP- $d_3$ ) were compared to a fully protonated sample (Figure 6), thus revealing trivial intramolecular P– $\text{CH}_3$  (blue) and P– $\text{OCH}_3$  (red) contact peaks. Clearly, the peak at  $\delta(^1\text{H}) = 6.7$  ppm reflects spatial proximity of matrix protons (bisphenol A) and the fortifier (cf. Figure 1). Nevertheless, in order to verify that the peak does not reflect hydroxyl protons obtained upon ring-opening (which in principle could be considerably shifted to higher ppm due to hydrogen bonding), a resin cured with deuterated amines was also measured. It yields the same contact peaks as the fully protonated sample thereby approving spatial proximity of the phosphonate to bisphenol A moieties, in accordance with the 2D  $^1\text{H}$  DQ correlation experiment (cf. Figure 3).

**4.3. Chemical Shift Computations.** Since the  $^{13}\text{C}$  and  $^{31}\text{P}$  chemical shifts of DMMP structural motifs change upon fortification, we explicitly considered the influence of the bisphenol A moiety on the NMR chemical shifts of the fortifier molecules by computing the magnetic response field

induced by this aromatic fragment. According to the obtained NICS map (which has been previously used to investigate both host–guest interactions<sup>66</sup> and packing behavior of liquid crystalline phases<sup>67</sup> (illustrated in Figure 7)) any nucleus located at the closest possible position to the bisphenol A moiety will experience  $\pi$ -shift no larger than 2.5–3.0 ppm, suggesting that the observed chemical shift changes in case of DMMP mainly result from *chemical modifications* upon curing of the resin. Since DMMP (apart from its commercial use as flame retardant) can be used as mild methylating reagent of, e.g., carboxylic acids and (preferably aromatic) amines, yielding the anion methyl methyl phosphonate (MMP),<sup>68</sup> we considered a DMMP fortified resin whose curing process was stopped after gelation (precure at 50 °C for 3 h).

As expected, the resulting resin has a reduced glass transition temperature of  $T_{\text{G}} = 70$  °C (fully cured:  $T_{\text{G}} = 99$  °C) while its  $^{31}\text{P}$  MAS NMR spectrum (Figure 8) clearly displays *two* resonances at 22.7 and 33.1 ppm, respectively, with an integrated area ratio of about 2:3. The signal at 22.7 ppm (MMP) is typically found for fully cured resins whereas the peak at 33.1 ppm is attributed to yet unreacted DMMP (based on the fact that the  $^{31}\text{P}$  chemical shift of DMMP dissolved in DMSO is 34.0 ppm). This assignment is further corroborated by a resin fortified with methyl methylphosphonic acid (MMPA), i.e., protonated MMP, which displays a broad signal around 22.7 ppm, thus indicating a similar phosphorus species compared to a DMMP fortified resin. While both DMMP and DMSO fortified resins are transparent and appear to form a homogeneous phase (at least upon eye inspection), MMPA fortified resin is *not*. Rather, upon mixing of the polymer monomers, MMPA forms a salt with the amines (extender, cross-linker) that precipitates from the solution thereby preventing a uniform distribution of the monomers. This observation suggests that DMMP apparently possesses a beneficial reactivity as it reacts slow enough to ensure homogeneous mixing of the monomer components and at the same time fast enough to avert prolonged curing of the resin.

The  $^{31}\text{P}$  chemical shift of MMP anions within the cavity (based on the averaged absolute chemical shieldings of 40 randomly sampled snapshots along a CPMD trajectory of the “non-branched” model) was computed 13 ppm *lower* than the corresponding  $^{31}\text{P}$  chemical shift of an isolated DMMP molecule (reference CPMD simulation), which is in good agreement with the experimental observations ( $\Delta\delta \approx -11$  ppm). Most notably, the experimentally observed trend of the  $^{31}\text{P}$  chemical shift cannot be reproduced by mere salt formation (i.e., simple MMP anion) without attributing additional screening effects of the host including weak hydrogen-bonding interactions, as demonstrated in case of the “ionic liquid” where  $\Delta\delta(^{31}\text{P}) \approx -24$  ppm was computed.

**4.4.  $^{15}\text{N}$  NMR.** Since conversion of DMMP into MMP during the postcure yields ammonium ions, resins were cured with  $^{15}\text{N}$ -labeled ethylenediamine in order to identify the presence of such species with a sufficient signal-to-noise ratio within reasonable NMR time. Indeed, the  $^{15}\text{N}$  CPMAS spectrum of DMMP fortified resin (Figure 9a) exhibits a broad peak at –353.4 ppm (reflecting major parts of the cross-linked resin) in addition to two fairly small resonances at –321.2 and –326.7 ppm, respectively, that are *absent* in the corresponding  $^{15}\text{N}$  CPMAS spectra of either unfortified or DMSO fortified resin. Notably, the  $^{15}\text{N}$  CPMAS spectrum of an only precured DMMP fortified resin shows the two additional resonances with weak intensity. Therefore, the two minor peaks are assigned to differently substituted ammonium ions (i.e., bearing one or two methyl groups

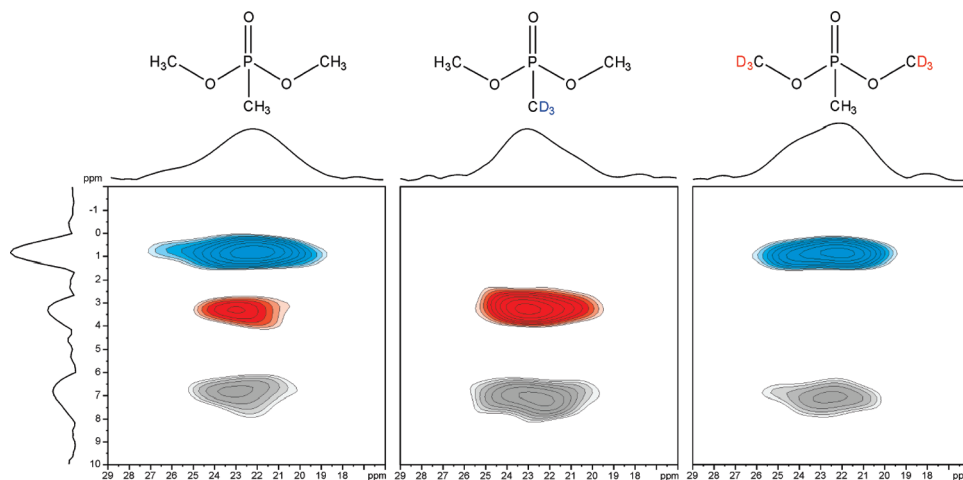


**Figure 6.**  $^1\text{H}$ – $^{31}\text{P}$  REPT–HSQC spectra at 700.1 MHz ( $^1\text{H}$ )/283.4 MHz ( $^{31}\text{P}$ ) and 29762 Hz MAS of a fully protonated DMMP fortified sample (left), a resin fortified with dimethyl methyl- $d_3$  phosphonate (middle) and dimethyl- $d_6$  methylphosphonate (right). All spectra were acquired using a Bruker Avance 700 machine equipped with a commercially available Bruker 2.5 mm double-resonance MAS probe. A total of 64  $t_1$  increments at steps of 33.6  $\mu\text{s}$  and 256 transients per increment at a relaxation delay of 5 s have been added employing the States-TPPI<sup>60</sup> method for phase sensitive detection.  $\pi/2$ -pulse lengths were of 2.5  $\mu\text{s}$  for  $^1\text{H}$  and  $^{31}\text{P}$  and a recoupling time of  $4\tau_{\text{R}} \approx 0.13$  ms was applied. Then 11 positive contour levels between 15% and 95% of the maximum peak intensity were plotted; the F2 projection is shown on the top.

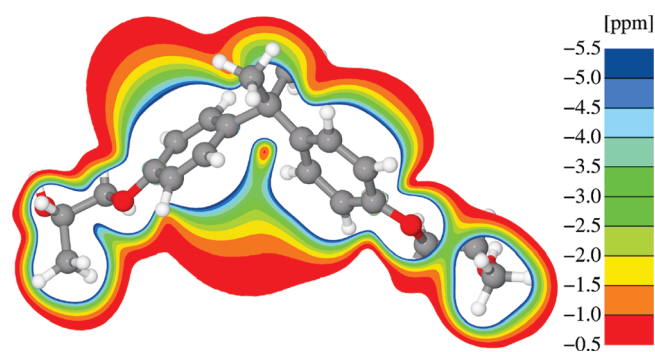


**Figure 7.** Calculated NICS map of a simplified model system representing a “non-branched” polymer fragment.

thereby reflecting nonbranched or branched nitrogens) that increase in intensity with proceeding demethylation of DMMP while the possible presence of *protonated* tertiary amines can be excluded. Though upon reaction of DMMP with secondary or primary amines, methyl methyl phosphonic acid (MMPA) may be formed as an intermediate, it is most probably deprotonated in the presence of excess amines. Protonated amines, however, are known to react readily with epoxy rings, thus rendering their existence in the cured resin very unlikely.<sup>69</sup> In contrast, at precure conditions (50 °C), uncharged tertiary amines such as those formed during cure (that comprise the polymer backbone) do *not* open epoxy rings.<sup>70</sup> This was checked by adding either triethylamine or triethylamine hydrochloride to an excess of Epon 825 (the epoxy precursor), where only the latter readily reacted at 50 °C. Also, further experiments with triethylamine indicate that DMMP does not methylate tertiary amines at this temperature. In conclusion, the polymer backbone gets only charged by the reaction of protonated amines with epoxy rings until the start of the postcure at 110 °C (Figure 9b).

**4.5. Deuteron NMR.** The relative strengths or impact of molecular or electrostatic interactions of the respective fortifier with the polymer host can be conveniently assessed by probing local dynamics of the fortifier molecules. Specifically, the deuteron is a spin-1 quadrupolar nucleus where the interaction of the nuclear quadrupole moment with a local

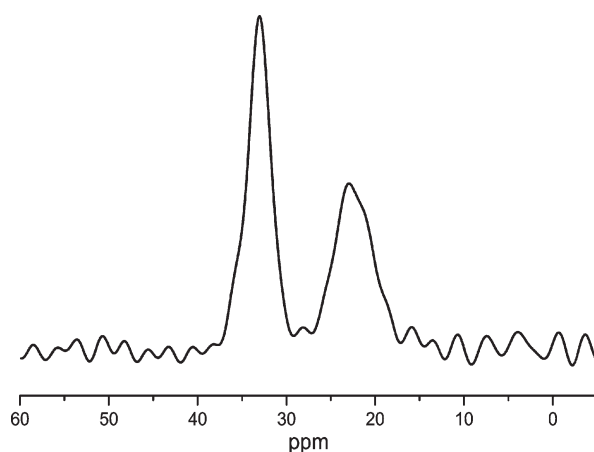


**Figure 8.**  $^{31}\text{P}$  CPMAS spectrum of a precured (3 h at 50 °C) DMMP fortified resin at 202.45 MHz and 25 kHz MAS using a Bruker DSX 500 machine, a contact time of 250  $\mu\text{s}$  coadding 256 transients;  $\pi/2$ -pulse length of 2.5  $\mu\text{s}$  and a recycle delay of 5 s. The contact time was held short to ensure polarization transfer originating from the methyl group directly bound to phosphorus only. Under such conditions, the intensity of both resonances should be approximately proportional to the number of phosphorus spins. This leads to an estimated DMMP conversion of 40%.

electric field gradient around the  $^2\text{H}$  nucleus of interest is very sensitive to molecular reorientations due to motions, thus providing orientation-dependent splittings of the line shape.<sup>71</sup> The rate and possible geometries of underlying motions may be extracted via matching of experimentally observed spectral lineshapes with computed lineshapes that result from a given model.<sup>72,73</sup>

Though in difficult cases experimental lineshapes may be reproduced by several distinct models,<sup>74</sup>  $^2\text{H}$  NMR still provides a fairly easy access to local geometries of mobile species.<sup>75</sup> In cases where more than one deuteron site is considered, improved spectral resolution and substantial gain in signal-to-noise can be achieved with  $^2\text{H}$  MAS NMR. Under slow MAS, the envelope of the respective spinning sideband pattern reflects the static line shape and in case of known geometries allows for extraction of dynamic rates (and hence, molecular correlation times).<sup>71</sup>

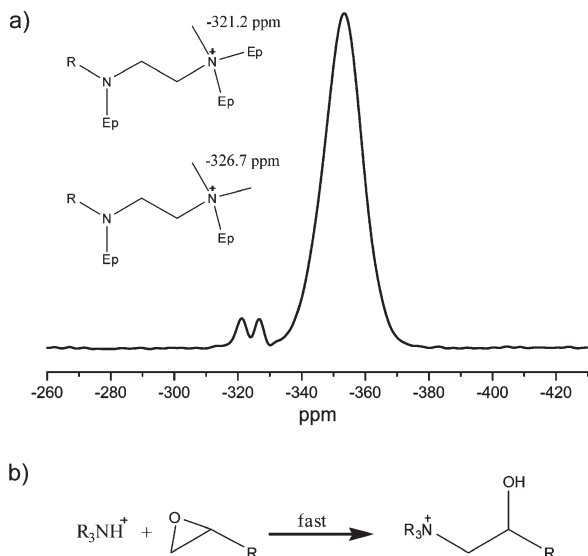


**Figure 9.** (a)  $^{15}\text{N}$  CPMAS spectrum of DMMP fortified resin cured with  $^{15}\text{N}$ -labeled ethylene diamine. Schematic structures of the respective polymer backbone cutouts are given: Ep denotes the polymer backbone and R aliphatic residues (cf. Scheme 2). The spectra were acquired at 30.42 MHz using a Bruker Avance II 300 machine with a contact time of 3 ms, coadding 45056 transients. The experiments were carried out using a Bruker 4 mm double resonance MAS probe spinning at 10 kHz,  $\pi/2$ -pulse length of 4.0  $\mu\text{s}$  and a recycle delay of 6 s. (b) Schematic reaction of a protonated tertiary amine, as it is formed in the polymer matrix after intermediate formation of MMPA during cure, with an epoxy ring. This reaction is faster than ring-opening with an unprotonated tertiary amine.

Since the width of MAS spinning sidebands is sensitive to exchange broadening, dynamic heterogeneities may be more easily identified under MAS conditions, but generally, motional broadening cannot be undone by MAS. If the inverse correlation time of the considered molecular motion (that is the jump rate of the C–D bond between different sites or orientations) approaches the MAS rate, both interfere and the line shape substantially broadens. When the rate of reorientation of the C–D bonds can be described by a rather narrow distribution function (like in case of well-defined motions),<sup>76</sup> even complete loss of signal intensity can be observed. In contrast, rather ill-defined motions that are reflected by a large distribution of correlation times where only a small fraction of C–D bonds fulfills the interference condition, yield only moderate line broadening.<sup>77</sup> In fact, the latter is observed in variable temperature  $^2\text{H}$  MAS NMR spectra of both DMMP- $d_3$  and DMSO- $d_6$  fortified resins at temperatures slightly below  $T_G$  ( $\approx 50$  °C for DMSO- $d_6$  and around 100 °C for DMMP- $d_3$ ) of the respective resin (see Supporting Information).

While only one peak at 2.1 ppm is observed for DMSO- $d_6$ , the corresponding  $^2\text{H}$  MAS NMR spectrum of dimethyl methyl- $d_3$  phosphonate at  $-20$  °C (Figure 10) reveals *two* distinct deuteron resonances at 2.0 and 0.1 ppm, respectively, with an integrated area ratio of  $\approx 1.1:1$ , thus indicating *two* inequivalent phosphonate species in the resin, which is in good agreement with the previously observed splitting of the P–CH<sub>3</sub> resonances in the  $^1\text{H}$ – $^{13}\text{C}$  REPT–HSQC spectrum of a DMMP fortified resin. Notably, at higher temperatures, both peaks collapse to a single line at an averaged chemical shift of 1.0 ppm.

Similar to  $^2\text{H}$  MAS NMR spectra, the static  $^2\text{H}$  NMR line shape is governed by the orientation of the individual C–D bond directions relative to the external magnetic

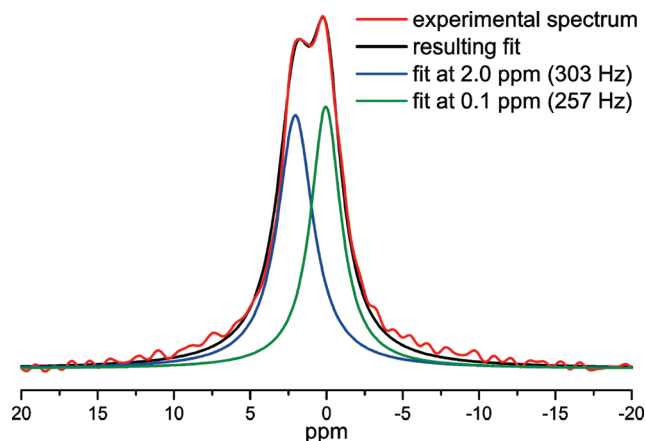


**Figure 10.**  $^2\text{H}$  MAS NMR spectrum of dimethyl methyl- $d_3$  phosphonate fortified resin at 107.5 MHz, 29762 Hz MAS, and  $-20$  °C. The line shape was deconvoluted with DMFit<sup>78</sup> yielding two Lorentzian lines at 0.1 and 2.0 ppm, respectively, with comparable linewidths of 303 Hz (blue) and 257 Hz (green).

field. The angular dependent quadrupolar coupling is then given by

$$\omega = \omega_L \pm \frac{1}{2} \omega_Q (3 \cos^2 \theta - 1 - \eta \sin^2 \theta \cos^2 \varphi) \quad (1)$$

where  $\omega_L$  is the Larmor frequency including the isotropic chemical shifts and  $\omega_Q$  denotes the strength of the quadrupolar coupling. The asymmetry parameter  $\eta$  describes the deviation from axial symmetry while the angles  $\theta$  and  $\varphi$  are the polar angles of the magnetic field  $B_0$  in the principal axes system of the quadrupolar coupling tensor. For rigid C–D bonds, its unique axis is along the C–D direction. In a powder, the maximum frequency splitting of the singularities is then  $\omega_Q \approx 2\pi \times 128$  kHz. However, in the presence of rapid molecular motion, the quadrupolar interaction can be partially averaged, thus yielding an averaged quadrupolar coupling tensor. Note that even in case of  $\eta = 0$ , the asymmetry parameter of the *averaged* tensor  $\eta$  can be unequal to zero. If molecular motion is present on a time scale in the order of the width of the spectrum (i.e., several kHz), lineshapes are dependent on both type and rate of the respective motion. It is crucial to note that only in the rigid and rapid exchange limit the spectra are identical to those obtained by a (hypothetical) conventional one-pulse experiment.<sup>27</sup> If the molecular motion approaches the intermediate exchange region, the application of the quadrupole echo is connected with a substantial loss of spectral intensity.

Deuteron solid state echo experiments<sup>79</sup> at temperatures ranging from  $-100$  to  $+60$  °C were recorded for both dimethyl methyl- $d_3$  phosphonate and dimethyl- $d_6$  sulfoxide fortified resins, respectively. Both show distinct differences with respect to the onset of motion and the development of the line shape with increasing temperature. In both cases, preaveraging of the quadrupolar coupling tensor due to rapid axial rotation of the P–CH<sub>3</sub> and S–CH<sub>3</sub> groups is observed yielding a frequency splitting of  $\omega_Q \approx 2\pi \times 43$  kHz ( $\approx 1/3$  of the rigid limit). Notably, only the width of the static pattern is reduced, not the shape.

For simulations of the  $^2\text{H}$  dynamic line shape, bond angles of DMSO were taken from literature data<sup>80</sup> while appropriate bond angles for MMP were derived from a DFT optimized model geometry (see below). Indeed, the obtained geometry depends on the level of theory but variances are typically in the order of  $\approx 1^\circ$  providing reasonable accuracy,

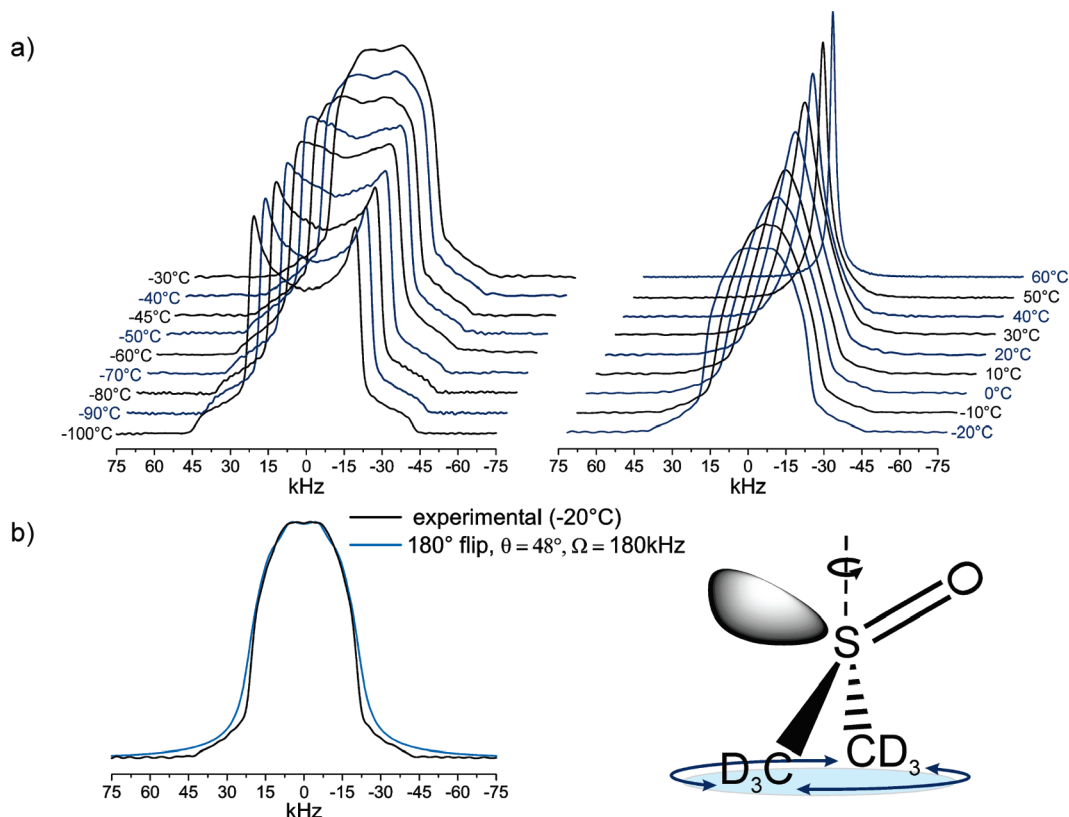


**Figure 11.** (a) Static variable temperature  $^2\text{H}$  solid echo measurements of DMSO- $d_6$  fortified resin at 76.8 MHz. A total of 3072 scans were taken at a relaxation delay of 0.5 s using an echo delay of 20  $\mu\text{s}$  and a  $\pi/2$ -pulse width of 5  $\mu\text{s}$ . (b) Comparison of experimental data obtained at  $-20^\circ\text{C}$  with simulated spectrum. Simulation is shown for a cone opening angle of  $48^\circ$  at a hopping rate of  $\Omega = 180$  kHz for the methyl groups. At  $-20^\circ\text{C}$  both “horns” of the rigid limit spectrum start to collapse into one line that further narrows at higher temperatures.

particularly with respect to the distribution of local environments of the respective additive in the resin.

All  $^2\text{H}$  NMR line shape simulations were conducted using the NMR-WEPLAB.<sup>75</sup> In case of DMSO- $d_6$ , line shape deconvolution based on the simple 2-site jump model on a single cone assuming a  $180^\circ$  flip angle around an axis centered between both S–C bonds (Figure 11) sufficiently reproduced the experimental data, where the applied cone opening angle of  $\approx 48^\circ$  is slightly smaller than expected for an ideal tetrahedron ( $54.8^\circ$ ). A possible distribution of motional correlation times reflecting different local environments of DMSO- $d_6$  in the resin was accounted for by applying a Lorentzian broadening of 5 kHz when fitting the experimental data. For a well-defined local jump motion the mean exchange rate ( $\langle\Omega\rangle$ ) is expected to follow an Arrhenius-type law

$$\langle\Omega\rangle = \Omega_\infty e^{-\langle E_A\rangle/RT} \quad (2)$$

where  $\Omega_\infty$  denotes the exchange rate at infinite temperature.  $\langle E_A\rangle$  is the mean activation energy for the center of the distribution and (according to (3)) may be obtained from the slope of a plot of  $\ln\langle\Omega\rangle$  vs the inverse temperature

$$\ln\langle\Omega\rangle = \ln\Omega_\infty - (\langle E_A\rangle/R) \times 1/T \quad (3)$$

In case of DMSO- $d_6$ , this analysis yields a mean activation energy of 20.3 kJ/mol, which is almost identical to the previously reported activation energy of the well-known methyl rotation in DMSO<sup>81</sup> rendering significant interactions between DMSO and the resin unlikely. For comparison,  $^2\text{H}$  solid echo spectra of pristine, frozen DMSO- $d_6$  at

temperatures ranging from  $-120$  to  $+20^\circ\text{C}$  (melting point:  $18^\circ\text{C}$ ) were recorded in steps of  $10^\circ\text{C}$ . In contrast to DMSO- $d_6$  included in the epoxy resin, the  $^2\text{H}$  line shape resembles a Pake pattern at all temperatures indicating the absence of extensive motion. In conclusion, this finding supports a mere filling of free volume of DMSO in the resin (similar to host–guest inclusion), where the absence of hydrogen bonding allows for a free molecule behavior of DMSO.

In the case of dimethyl methyl- $d_3$  phosphonate (DMMP- $d_3$ ) fortified resin, the experimental lineshapes cannot be reproduced with a single type of motion (Figure 12). At least two sets of PAKE pattern have to be considered, which indeed is consistent with the likely presence of two different phosphonate species already identified (see above). It can be readily seen from a direct comparison of the corresponding  $^2\text{H}$  solid echo spectra of both DMSO- $d_6$  and DMMP- $d_3$  fortified resin that the onset of an additional motion (other than mere methyl rotation) in case of DMMP- $d_3$ , as indicated by characteristic line shape changes, occurs at considerably higher temperature ( $\Delta T = 60^\circ\text{C}$ ) than observed for DMSO- $d_6$ , probably reflecting rather strong (electrostatic) interactions between the fortifier and the resin (recall that demethylation of DMMP upon curing yields charged species). The simplest model that accounts for two different phosphonate species while satisfactorily reproducing the experimental lineshapes comprises a superposition of two patterns where one reflects a rather rigid fraction with  $\omega_Q \approx 2\pi \times 42.6$  kHz while in case of the more mobile fraction, further averaging of the quadrupolar coupling is achieved by fairly small angle oscillations (“wobbling”) around the P=O axis. At higher temperatures, the fraction of the mobile species increases at expense of the rigid fraction until around

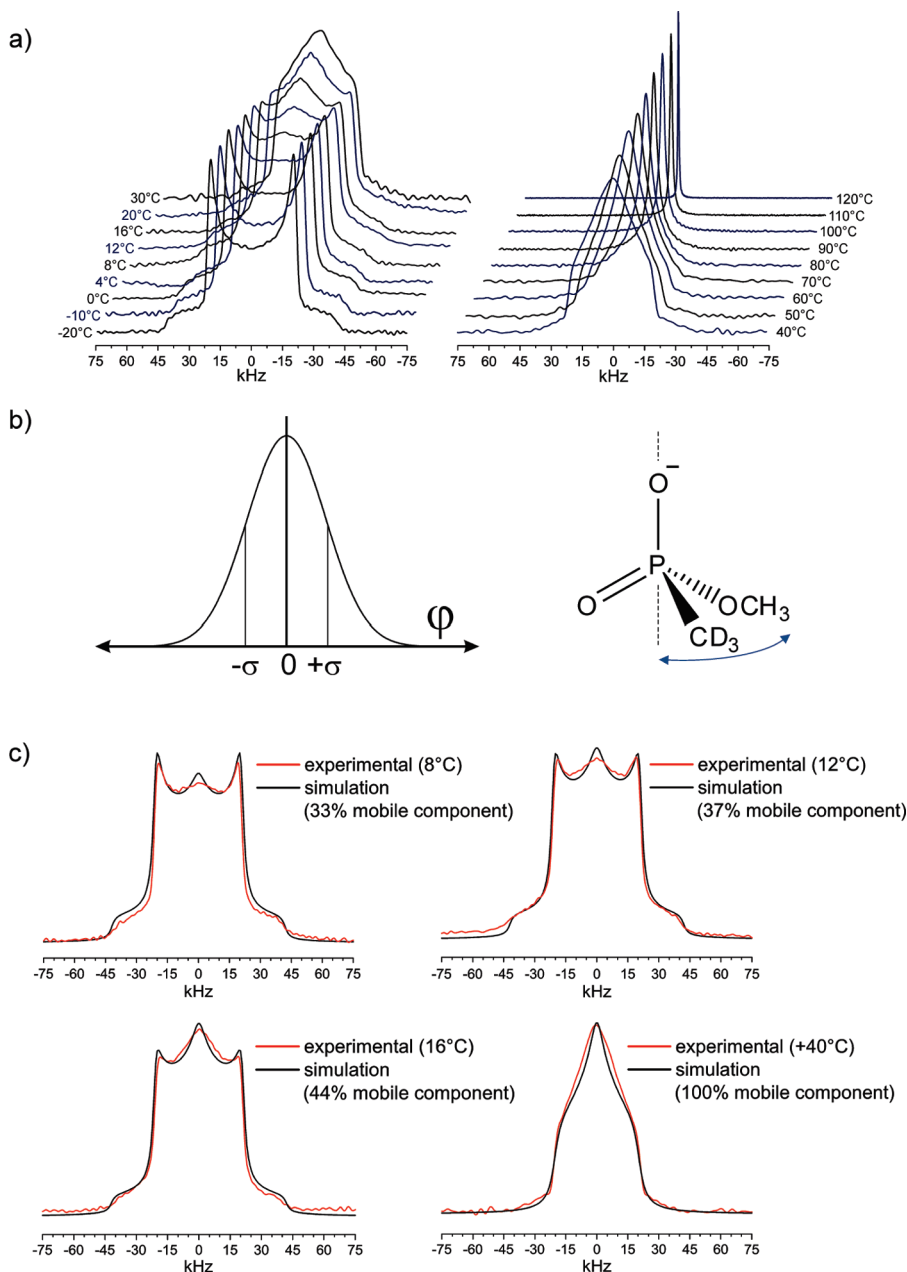


**Figure 12.** (a) Variable temperature  $^2\text{H}$  solid echo measurements of dimethyl methyl- $d_3$  phosphonate fortified resin at 76.8 MHz. 3072 scans were taken at a relaxation delay of 0.5 s using an echo delay of  $20\ \mu\text{s}$  and a  $\pi/2$ -pulse width of  $5\ \mu\text{s}$ . Characteristic line shape distortions occur in the range from  $+8\ ^\circ\text{C}$  to approximately  $+70\ ^\circ\text{C}$  before an isotropic line is observed at higher temperatures. (b) Schematic model illustrating the “wobbling” motion. Mathematically, this is described by a jump angle of  $360^\circ \pm \varphi$ , where  $\varphi$  is an angle described by a Gaussian distribution with  $2\sigma = 90^\circ$ . The cone opening angle is  $\theta = 71^\circ$ . Five kHz Lorentzian broadening was applied for the simulations. (c) Comparison of experimental data obtained at  $+8$ ,  $+12$ ,  $+16$ , and  $+40\ ^\circ\text{C}$  and simulated spectra, where the simulated spectra differ in the fraction of the mobile (“wobbling”) component.

$T_G$ , where isotropic tumbling accompanied by substantial line-narrowing is observed. As both subspectra arise from deuterons “hopping” either in the fast or static limit (i.e., the motion is either below or above the kHz regime), the respective fractions can be estimated from the area under the subspectra without further corrections.

**Aging of the Resin.** When the DSC measurements were repeated using approximately six months old own-synthesized samples as well as rather long-term stored samples from the previous study (kindly provided by M. Junk), the resulting glass transition temperature of both DMSO fortified and unfortified resin has decreased by only 3 and 4  $^\circ\text{C}$ , respectively. In contrast, both DMMP fortified resins revealed a substantial decrease of  $T_G$  very close to the  $T_G$  of an

unfortified resin, suggesting complete loss of fortification. However, the corresponding  $^1\text{H}$  and  $^{13}\text{C}$  (CP) MAS NMR spectra of the aged samples are virtually identical to the spectra of freshly prepared compounds indicating only minor (local) structural changes. Nevertheless, static variable temperature  $^2\text{H}$  solid echo spectra of a freshly synthesized DMMP- $d_3$  fortified resin exhibit very similar lineshapes compared to an aged resin except that for a given jump rate to be reached, the fresh resin has to be heated around 15  $^\circ\text{C}$  higher than the aged resin. This finding approves the validity of the fortifier jump model independent of the age of the resin, where reduced fortifier motion at a given temperature in the case of fresh resin indicates changes of the fortifier–epoxy network interactions upon aging. In order to possibly

rationalize this aging process, further work on phosphonate-based fortifier molecules is currently in progress.

## 5. Conclusion

Applying modern solid-state NMR techniques and *ab initio* DFT computations, we gained insight into the mechanism of molecular fortification of bisphenol A based amine cured model epoxy resins. In particular, we have demonstrated a “free molecule”-type behavior of DMSO in DMSO-fortified resins similar to common inclusion compounds such as carceplexes<sup>82</sup> thereby revealing mere filling of free volume by the additive. Nevertheless, van der Waals forces between both the resin and fortifier may weakly connect polymer backbone chains thereby mediating fortification. Furthermore, a minor decrease of local segmental polymer backbone motion is likely. In case of DMMP-fortified resins, however, chemical modification of the epoxy resin is observed, yielding the fortifier methyl methylphosphonate (MMP). Notably, methylation of amines during postcure partially proceeded to the formation of quaternary ammonium species thus introducing positive charges on the polymer backbone. Indeed, the onset of “wobbling” motion of MMP at rather high-temperatures and the likely presence of two different MMP species within the resin clearly reflect pronounced interactions of MMP with the resin, suggesting a complex mechanism of fortification. This is also evident in the lack of suppression of the  $\beta$ -relaxation transition which is in general observed for fortified polymer systems by dynamic mechanical analysis. The tentative suggestion of H-bonding as substantial contribution to the effect of fortification can be excluded for both fortifiers. Rather, electrostatic interactions between MMP and positively charged nitrogens keep both moieties in close spatial proximity (which could be regarded as further branching where MMP acts as short “side chain”) thus restricting the local motion of neighboring polymer moieties or apparently increasing the local cross-link density of the resin. Further investigations are required to rationalize both the observed loss of fortification upon aging and impact of salt formation on the fortification of epoxy resins.

**Supporting Information Available:** Figures showing additional DQ MAS and REPT-HSQC spectra not shown in the main text as well as complete ref 42. This material is available free of charge via the Internet at <http://pubs.acs.org>.

**Acknowledgment.** The authors thank Matthias Junk for providing reference samples from a previous study and Verona Maus and Andreas Hahnwald for technical support as well as Pawel Bednarek from the Informatikdienst der Universität Freiburg (Switzerland) for technical support.

## References and Notes

- Murphy, J. *Additives for Plastics Handbook*; Elsevier: Amsterdam, 2001.
- Zerda, A. S.; Lesser, A. J. *J. Appl. Polym. Sci.* **2002**, *84*, 302–309.
- Mijovic, J. *J. Appl. Polym. Sci.* **1990**, *40*, 845–865.
- Hata, N.; Kumanotani, J. *J. Appl. Polym. Sci.* **1977**, *21*, 1257–1266.
- Hata, N.; Yamauchi, R.; Kumanotani, J. *J. Appl. Polym. Sci.* **1973**, *17*, 2173–2181.
- Zerda, A. S.; Lesser, A. J. *Polym. Eng. Sci.* **2004**, *44*, 2125–2133.
- Daly, J.; Britten, A.; Garton, A.; McLean, P. D. *J. Appl. Polym. Sci.* **1984**, *29*, 1403–1414.
- Jackson, W. J., Jr.; Caldwell, J. R. *J. Appl. Polym. Sci.* **1967**, *11*, 227–244.
- Ueda, M. *Polym. Eng. Sci.* **2004**, *44*, 1877–1884.
- Anderson, S. L.; Grulke, E. A.; DeLassus, P. T.; Smith, P. B.; Kocher, C. W.; Landes, B. G. *Macromolecules* **1995**, *28*, 2944–2954.
- Guerrero, S. J. *Macromolecules* **1989**, *22*, 3480–3485.
- Maxwell, A. S.; Monnerie, L.; Ward, I. M. *Polymer* **1998**, *39*, 6851–6859.
- Calzia, K. J.; Forcum, A.; Lesser, A. J. *J. Appl. Polym. Sci.* **2006**, *102*, 4606–4615.
- Robeson, L. M. *Polym. Eng. Sci.* **1969**, *9*, 277–281.
- Maeda, Y.; Paul, D. R. *J. Polym. Sci., Part B: Polym. Phys.* **1987**, *25*, 1005–1016.
- Wang, Y.; Inglefield, P. T.; Jones, A. A. *J. Polym. Sci., Part B: Polym. Phys.* **2002**, *40*, 1965–1974.
- Lesser, A. J.; Calzia, K.; Junk, M. *Polym. Eng. Sci.* **2007**, *47*, 1569–1575.
- Robeson, L. M.; Faucher, J. A. *J. Polym. Sci., Part B* **1969**, *7*, 35–40.
- Reichert, D. *Annu. Rep. NMR Spectrosc.* **2005**, *55*, 159–203.
- White, J. L.; Wachowicz, M. *Annu. Rep. NMR Spectrosc.* **2008**, *64*, 189–209.
- Orendt, A. M.; Facelli, J. C. *Annu. Rep. NMR Spectrosc.* **2007**, *62*, 115–178.
- Liu, Y.; Roy, A. K.; Jones, A. A.; Inglefield, P. T.; Ogden, P. *Macromolecules* **1990**, *23*, 968–977.
- Heux, L.; Laupretre, F.; Halary, J. L.; Monnerie, L. *Polymer* **1998**, *39*, 1269–1278.
- Roy, A. K.; Inglefield, P. T.; Shibata, J. H.; Jones, A. A. *Macromolecules* **1987**, *20*, 1434–1437.
- Fischer, E. W.; Hellmann, G. P.; Spiess, H. W.; Hoerth, F. J.; Ecarious, U.; Wehrle, M. *Makromol. Chem., Suppl.* **1985**, *12*, 189–214.
- Schmidt, C.; Kuhn, K. J.; Spiess, H. W. *Prog. Colloid Polym. Sci.* **1985**, *71*, 71–76.
- Wehrle, M.; Hellmann, G. P.; Spiess, H. W. *Colloid Polym. Sci.* **1987**, *265*, 815–822.
- Maxwell, A. S.; Ward, I. M.; Laupretre, F.; Monnerie, L. *Polymer* **1998**, *39*, 6835–6849.
- Cauley, B. J.; Cipriani, C.; Ellis, K.; Roy, A. K.; Jones, A. A.; Inglefield, P. T.; McKinley, B. J.; Kambour, R. P. *Macromolecules* **1991**, *24*, 403–409.
- Bergquist, P.; Zhu, Y.; Jones, A. A.; Inglefield, P. T. *Macromolecules* **1999**, *32*, 7925–7931.
- Zhang, C.; Wang, P.; Jones, A. A.; Inglefield, P. T.; Kambour, R. P. *Macromolecules* **1991**, *24*, 338–340.
- Merritt, M. E.; Goetz, J. M.; Whitney, D.; Chang, C.-P. P.; Heux, L.; Halary, J. L.; Schaefer, J. *Macromolecules* **1998**, *31*, 1214–1220.
- Fukaya, Y.; Iizuka, Y.; Sekikawa, K.; Ohno, H. *Green Chem.* **2007**, *9*, 1155–1157.
- Schleyer, P. v. R.; Maerker, C.; Dransfeld, A.; Jiao, H.; Hommes, N. J. R. v. E. *J. Am. Chem. Soc.* **1996**, *118*, 6317–6318.
- (a) Geerlings, P.; De Proft, F.; Langenaeker, W. *Chem. Rev.* **2003**, *103*, 1793–1873. (b) Parr, R. G.; Yang, W. *Density Functional Theory of Atoms and Molecules*; Oxford University Press: Oxford, U.K., 1989.
- Harris, R. K. *Solid State Sci.* **2004**, *6*, 1025–1037.
- Hutter, J. et al. Computer code CPMD, version 3.9, 1990–2004, IBM Corp. and MPI-FKF Stuttgart, <http://www.cpmd.org>
- Becke, A. D. *Phys. Rev. A* **1988**, *38*, 3098–3100.
- Lee, C.; Yang, W.; Parr, R. G. *Phys. Rev. B* **1988**, *37*, 785–789.
- (a) Goedecker, S.; Teter, M.; Hutter, J. *Phys. Rev. B* **1996**, *54*, 1703–1710. (b) Hartwigsen, C.; Goedecker, S.; Hutter, J. *Phys. Rev. B* **1998**, *58*, 3641–3662.
- Sebastiani, D. *ChemPhysChem.* **2006**, *7*, 164–175.
- Frisch, M. J. et al. Gaussian 03 Revision D. 02; Gaussian, Inc.: Wallingford, CT, 2004. The complete reference is available in the Supporting Information.
- (a) Becke, A. D. *J. Chem. Phys.* **1993**, *98*, 5648–5652. (b) Stephens, P. J.; Devlin, F. J.; Chabalowski, C. F.; Frisch, M. J. *J. Phys. Chem.* **1994**, *98*, 11623–11627.
- Harpam, M. R.; Levinger, N. E.; Ladanyi, B. M. *J. Phys. Chem. B* **2008**, *112*, 283–293.
- Luzar, A.; Chandler, D. *J. Chem. Phys.* **1993**, *98*, 8160–8173.
- Geerke, D. P.; Oostenbrink, C.; Van der Vegt, N. F. A.; Van Gunsteren, W. F. *J. Phys. Chem. B* **2004**, *108*, 1436–1445.
- Vechi, S. M.; Skaf, M. S. *J. Chem. Phys.* **2005**, *123*, 154507/1–154507/8.
- Duer, M. J.; Rocha, J.; Klinowski, J. *J. Am. Chem. Soc.* **1992**, *114*, 6867–6874.
- Vishnyakov, A.; Neimark, A. V. *J. Phys. Chem. A* **2004**, *108*, 1435–1439.
- Ault, B. S.; Balboa, A.; Tevault, D.; Hurley, M. J. *Phys. Chem. A* **2004**, *108*, 10094–10098.
- (a) Khan, M.; Enkelmann, V.; Brunklaus, G. *J. Am. Chem. Soc.* **2010**, *132*, 5254–5263. (b) Brown, S. P.; Zhu, X. X.; Saalwächter, K.

- J. Am. Chem. Soc.* **2001**, *123*, 4275–4285. (c) Goward, G. R.; Sebastiani, D.; Schnell, I.; Spiess, H. W.; Kim, H. D.; Ishida, H. *J. Am. Chem. Soc.* **2003**, *125*, 5792–5800. (d) Schnell, I.; Langer, B.; Soentjens, S. H. H.; Sijbesma, R. P.; van Genderen, M. H. P.; Spiess, H. W. *Phys. Chem. Chem. Phys.* **2002**, *4*, 3750–3758.
- (52) Chierotti, M. R.; Gobetto, R. *Chem. Commun.* **2008**, *14*, 1621–1634.
- (53) Khan, M.; Brunklaus, G.; Enkelmann, V.; Spiess, H. W. *J. Am. Chem. Soc.* **2008**, *130*, 1741–1748.
- (54) Gobetto, R.; Nervi, C.; Valfrè, E.; Chierotti, M. R.; Braga, D.; Maini, L.; Grepioni, F.; Harris, R. K.; Ghi, P. Y. *Chem. Mater.* **2005**, *17*, 1457–1466.
- (55) Brown, S. P. *Prog. Nucl. Magn. Reson.* **2007**, *50*, 199–251.
- (56) (a) Bolz, I.; Moon, C.; Enkelmann, V.; Brunklaus, G.; Spange, S. *J. Org. Chem.* **2008**, *73*, 4783–4793. (b) Ben Shir, I.; Kababya, S.; Amitay-Rosen, T.; Balazs, Y. S.; Schmidt, A. J. *Phys. Chem. B* **2010**, *114*, 5989–5996. (c) Zienau, J.; Kussmann, J.; Koziol, F.; Ochsenfeld, C. *Phys. Chem. Chem. Phys.* **2007**, *9*, 4552–4562. (d) Goobes, G.; Stayton, P. S.; Drobny, G. P. *Prog. Nucl. Magn. Reson.* **2007**, *50*, 71–85. (e) Ochsenfeld, C.; Koziol, F.; Brown, S. P.; schaller, T.; Seelbach, U. P.; Klarner, F. G. *Solid State Nucl. Magn. Reson.* **2002**, *22*, 128–153.
- (57) Schulz-Dobrick, M.; Schnell, I. *Central Eur. J. Chem.* **2005**, *3*, 245–251.
- (58) Bradley, J. P.; Tripon, C.; Filip, C.; Brown, S. P. *Phys. Chem. Chem. Phys.* **2009**, *11*, 6941–6952.
- (59) Geen, H.; Titman, J. J.; Gottwald, J.; Spiess, H. W. *Chem. Phys. Lett.* **1994**, *227*, 79–86.
- (60) Marion, D.; Ikura, M.; Tschudin, R.; Bax, A. *J. Magn. Reson.* **1989**, *85*, 393–399.
- (61) Gottlieb, H. E.; Kotlyar, V.; Nudelman, A. *J. Org. Chem.* **1997**, *62*, 7512–7515.
- (62) (a) Lazzeretti, P. *Prog. Nucl. Magn. Reson. Spectrosc.* **2000**, *36*, 1–88. (b) Gomes, J. A. N. F.; Mallion, R. B. *Chem. Rev.* **2001**, *101*, 1301–1315.
- (63) Saalwächter, K.; Spiess, H. W. *J. Chem. Phys.* **2001**, *114*, 5707–5728.
- (64) Saalwächter, K.; Graf, R.; Spiess, H. W. *J. Magn. Reson.* **2001**, *148*, 398–418.
- (65) Levitt, M. H. *Encycl. Nucl. Magn. Reson.* **2002**, *9*, 165–196.
- (66) (a) Brunklaus, G.; Koch, A.; Sebastiani, D.; Spiess, H. W. *Phys. Chem. Chem. Phys.* **2007**, *9*, 4545–4551. (b) Hoffmann, A.; Sebastiani, D.; Sugiono, E.; Yun, S.; Kim, K. S.; Spiess, H. W.; Schnell, I. *Chem. Phys. Lett.* **2004**, *388*, 164–169. (c) Brouwer, D. H.; Alavi, A.; Ripmeester, J. A. *Phys. Chem. Chem. Phys.* **2008**, *10*, 3857–3860. (d) Moon, C.; Brunklaus, G.; Sebastiani, D.; Rudzevich, Y.; Böhmer, V.; Spiess, H. W. *Phys. Chem. Chem. Phys.* **2009**, *11*, 9241–9249.
- (67) Hansen, M. R.; Graf, R.; Sekharan, S.; Sebastiani, D. *J. Am. Chem. Soc.* **2009**, *131*, 5251–5256.
- (68) Sutter, P.; Weis, C. D. *Phosphorus Sulfur* **1978**, *4*, 335–339.
- (69) Yang, C. P.; Ting, C. Y. *J. Appl. Polym. Sci.* **1993**, *49*, 1019–1029.
- (70) Galego, N.; Vazquez, A.; Williams, R. J. J. *Polymer* **1994**, *35*, 857–861.
- (71) Hologne, M.; J. Hirschinger, J. *Solid State Nucl. Magn. Reson.* **2004**, *26*, 1–10.
- (72) Schmidt-Rohr, K.; Spiess, H. W. *Multidimensional Solid-State NMR and Polymers*: Academic Press: London, 1994.
- (73) Macho, V.; Brombacher, L.; Spiess, H. W. *Appl. Magn. Reson.* **2001**, *20*, 405–432.
- (74) Lee, Y. J.; Murakhtina, T.; Sebastiani, D.; Spiess, H. W. *J. Am. Chem. Soc.* **2007**, *129*, 12406–12407.
- (75) Cutajar, M.; Ashbrook, S. E.; Wimperis, S. *Chem. Phys. Lett.* **2006**, *423*, 276–281.
- (76) Spiess, H. W. *Adv. Polym. Sci.* **1985**, *66*, 24–56.
- (77) Brunklaus, G.; Schauf, S.; Markova, D.; Klapper, M.; Müllen, K.; Spiess, H. W. *J. Phys. Chem. B* **2009**, *113*, 6674–6681.
- (78) Massiot, D.; Fayon, F.; Capron, M.; King, I.; Le Calve, S.; Alonso, B.; Durand, J.-O.; Bujoli, B.; Gan, Z.; Hoatson, G. *Magn. Reson. Chem.* **2002**, *40*, 70–76.
- (79) Powles, J. G.; Strange, J. H. *Proc. Phys. Soc., London* **1963**, *82*, 6–15.
- (80) Typke, V.; Dakkouri, M. *J. Mol. Struct.* **2001**, *599*, 177–193.
- (81) Ripmeester, J. A. *Can. J. Chem.* **1981**, *59*, 1671–1674.
- (82) Kurdistani, S. K.; Robbins, T. A.; Cram, D. J. *J. Chem. Soc., Chem. Commun.* **1995**, 1259–1260.